Effect of Successive Heat Treatment on the Performance of Superconducting Radio Frequency Niobium Cavities

B. D. Khanal and P. Dhakal

Journal of Nepal Physical Society
Volume 8, No 2, 2022
(Special Issue: ANPA Conference 2022)
ISSN: 2392-473X (Print), 2738-9537 (Online)

JNPS, **8** (2), 53-58 (2022)
DOI: http://doi.org/10.3126/jnphyssoc.v8i2.50152

Published by: Nepal Physical Society
P.O. Box: 2934
Tri-Chandra Campus
Kathmandu, Nepal
Email: nps.editor@gmail.com

ANPA Conference 2022
ISSN : 2392-473X(Print), 2738-9537 (Online)

DOI:http://doi.org/10.3126/jnphyssoc.v8i2.50152

Effect of Successive Heat Treatment on the Performance of Superconducting Radio Frequency Niobium Cavities

B. D. Khanal[1] and P. Dhakal[2, a)]

[1)]*Department of Physics, Old Dominion University, Norfolk, VA 23529, USA*
[2)]*Thomas Jefferson National Accelerator Facility, Newport News VA 23606, USA*

[a)]*Corresponding author: dhakal@jlab.org*

Abstract. One of the primary sources of radio frequency residual losses leading to lower quality factor is trapped residual magnetic field during the cooldown of superconducting radio frequency cavities. It has been reported that non-uniform recrystallization of niobium cavities after the post fabrication heat treatment leads to higher flux trapping during the cooldown, and hence the lower quality factor. Here, we fabricated two 1.3 GHz single cell cavities from high purity fine grain niobium and processed with successive heat treatments in the range 800-1000 °C to measure the flux expulsion and flux trapping sensitivity. The result indicates that although flux expulsion improves with increased heat treatments, there is a noticeable difference between the flux trapping sensitivity depending on the cavity. Evaluation of microstructure maybe crucial to understand the impact of flux trapping sensitivity on cavity performance.

Received:15 September 2022; **Accepted**: 12 October 2022; **Published**: 31 December 2022

Keywords: SRF cavities; High Q_0; Flux expulsion and trapping.

INTRODUCTION

Superconducting radio frequency (SRF) cavities are the technology of choice for modern particle accelerators. The energy is stored in the form of electromagnetic field and nearly all energy is transferred to the charge particles to accelerate close to the velocity of light. The benefits of using superconducting niobium (Nb) to fabricate cavities are due to low power dissipation on cavity walls. The shape and size of SRF cavities varies depending on the applications. The elliptical cavities used to accelerate electrons or protons are excited in TM_{010} mode where the electric field is concentrated along the center of the cavity whereas magnetic field is higher on cavity walls. The performance of SRF cavities are measured in terms of quality factor (Q_0) as a function of accelerating gradient, E_{acc}. The quality factor is defined as the ratio of energy stored (U) to the energy dissipation (P_d) per rf cycle as:

$$Q_0 = \frac{\omega U}{P_d}. \tag{1}$$

The energy store on cavity is given by

$$U = \frac{\mu_0}{2}\int |\vec{H}|^2 dV \tag{2}$$

where H is the magnetic field in the cavity and μ_0 is the permeability of free space. The power dissipated is given by the integral of wall losses over its surface as:

$$P_d = \frac{R_s}{2}\int |\vec{H}|^2 dS \tag{3}$$

where R_s is the surface resistance. The quality factor can be written as

$$Q_0 = \frac{G}{R_s} \tag{4}$$

where,

$$G = \frac{\omega\mu_0 \int |\vec{H}|^2 dV}{\int |\vec{H}|^2 dS} \tag{5}$$

defined as the geometric factor and depends on the cavity shape. The high quality factor can be achieved by minimizing the surface resistance [1]. High quality factor in SRF cavities is not only limited to particle accelerators but also emerging as an application to quantum computing and quantum information science [2-6] .

Unlike the dc surface resistance in a superconductor, the rf surface resistance in SRF cavities is the sum of temperature independent part, commonly known as residual

resistance (R_i) and temperature dependent BCS resistance (R_{BCS}). The R_i arise due to several intrinsic and extrinsic factor and R_{BCS} is the result of rf dissipation by unpaired quasi-particles in superconductors and is explained by BCS theory of superconductivity [7, 8].

One of the significant contributing factors to residual resistance is the trapped magnetic flux due to the insufficient flux expulsion of an ambient magnetic field from the SRF cavities when cavities cool down through the superconducting transition temperature [9-14] . According to Meissner effect, all magnetic flux is supposed to be expelled from the bulk of the superconductor during the superconducting phase transition. However, the microstructural defects, dislocations, and impurities provide favorable sites for the magnetic flux pinned in terms of the vortices, which contributes to an additional rf loss when exposed to the field [15]. It has been demonstrated that several different pinning mechanisms plays a vital role to the rf losses due to vortices [16]. Studies showed that the impurity doped cavities are even more vulnerable to the vortices dissipation due to the presence of the dopant on cavities rf surface [17-20]. Earlier studies on flux expulsion and rf losses due to the pinned vortices showed that better flux expulsion can be achieved when the cavity annealing temperature is increased while surface treatment has minimal effect [21]. The higher quality factor can be achieved with better flux expulsion when all the other conditions are kept same. However, the nature of pinning depends on the amount of flux being trapped on the bulk of niobium cavities and eventually affecting the optimal quality factor [15, 16].

The increase in annealing temperature minimizes the pinning centers by removing the cluster of impurities and dislocations. In addition, the metallurgical state with larger grain size is expected as the annealing temperature is increased [21]. The fine-grain recrystallized microstructure with an average grain size of 10–50 μm leads to flux trapping even with a lack of dislocation structures in grain interiors and larger grain sizes beyond 100–400 μm do not lead to preferential flux trapping, as observed directly by magneto-optical imaging [22]. In order to obtain repeatable and consistent cavity performance and improve process control, it is important to understand the relationship between microstructure, flux trappig and eventual cavity performance. In this study, we have fabricated two 1.3 GHz single-cell Nb cavities from SRF grade Nb sheet from two different vendors. The flux expulsion, flux trapping sensitivity and rf performance in terms of quality factor as a function of accelerating gradient were measured after successive heat treatment in the temperature range of 800 – 1000 °C.

CAVITY'S SURFACE PREPARATIONS

We have fabricated two 1.3 GHz TESLA-shaped [23] single cell cavities: named as TCA-01, center-cell design [G=269.83 Ω, B_p/E_{acc}= 4.12 mT/(MV/m)] and TE1-05 end-cell design [G=277.85 Ω, B_p/E_{acc}= 4.23 mT/(MV/m)] from high purity fine grain niobium with residual resistivity ratio, RRR $\sim$ 400. Cavity TCA-01 was fabricated in-house at Jefferson Lab from the niobium provided by Tokyo Denkai and TE1-05 was fabricated at Zanon Research & Innovation Srl, Italy from the niobium provided by Ningxia OTIC, China. Standard cavity fabrication technique of deep drawing of half cell, trimming, electron beam welding to the beam tube made of reactor grade niobium was followed. After the fabrication, the cavities received $\sim$ 150 μm inner surface material removal by electropolishing (EP). The flux expulsion and rf measurements were made after successive heat treatments at 800, 900 and 1000 °C for 3 hours. After each heat treatments, cavities received $\sim$ 25 μm electropolishing as the final surface preparation before the rf test.

EXPERIMENTAL SETUP

Three flux-gate magnetometers (FGMs) were fixed at the equator about 120° apart each and six temperature sensors: two at top iris, two at equator and two at bottom iris about 180° apart each were fixed parallel to the cavity's surface as shown in Fig. 1(a); to measure the magnetic flux and temperature during the thermal cycles. Figure 1(b) shows the change in the flux measured by FGMs during the transition of normal state to superconducting state.

EXPERIMENTAL RESULTS

The experiment was performed to analyze the flux expulsion ratio by measuring the ratio of magnetic field after (B_{sc}) and before (B_n) the superconducting transition. The measurements were repeated by warming up the cavity above transition temperature and cooling again with different temperature difference between the cavity irises. The flux trapping sensitivity was measured by extracting the residual resistance from Q_0 vs T with different flux trapping conditions. The measurements were repeated after each successive heat treatments at 800, 900 and 1000 °C.

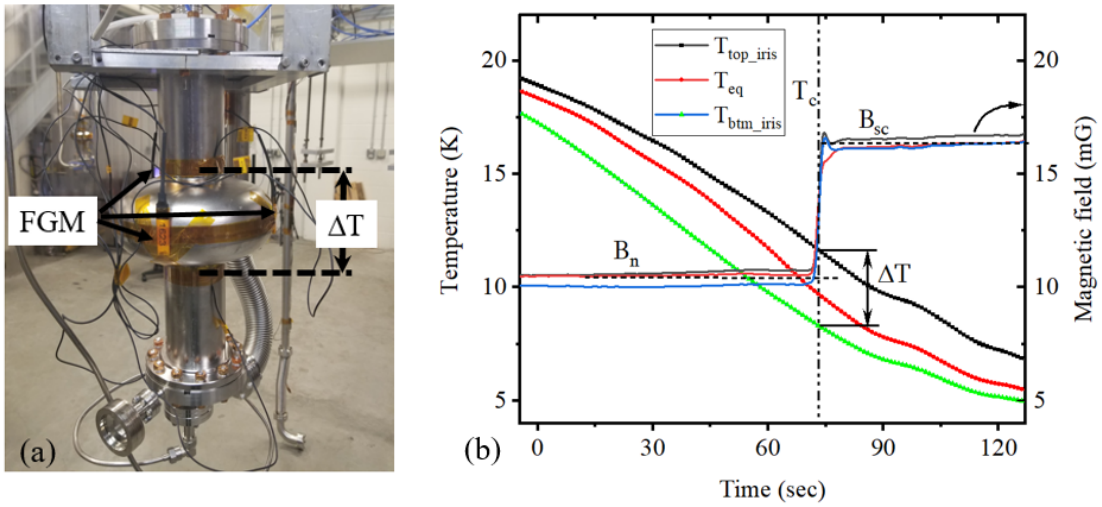

FIGURE 1. (a) Experimental set up for flux expulsion and rf measurements with FGMs and temperature sensors. (b) The change in magnetic flux measured by FGMs during the superconducting transition.The cooldown rate is $\sim$ 0.12 K/s.

Flux Expulsion

Figure 2. shows the flux expulsion ratio as a function of ΔT after different heat treatment. The ratio $B_{sc}/B_n = 1$ and $\sim$ 1.7 shows that the full flux trapping and full flux expulsion condition. Both cavities showed poor flux expulsion after 800 °C/3h heat treatment. However, both cavities showed strong flux expulsion with $B_{sc}/B_n \sim 1.6$ after 900 °C/3h and 1000 °C/3h heat treatment. The flux expulsion ratio is closer to full flux expulsion limit when ΔT is greater than 2.0 K.

RF Results and Flux Trapping Sensitivity

The Q_0 vs. the helium bath temperature (T) measurement was taken from 4.3 to 1.6 K at $B_p \sim 15$ mT. At 2.0 K, the Q_0 vs. E_{acc} measurement was carried out. The second set of measurements was made after warming the cavity above T_c and cooldown with $\sim$20 mG residual magnetic field in Dewar. The cavity was cooled with ΔT < 0.1 K ($B_{sc}/B_{nc} \sim 1$), ensuring that maximum ambient magnetic field was trapped during the cooldown. Again, the Q_0 vs. T measurement was repeated from 4.3 to 1.6 K and at 2.0 K, the Q_0 vs. E_{acc} measurement was done. This allows us to extract the flux trapping sensitivity; the increase in residual resistance per mG of trapped residual magnetic field during cooldown. The R_s (G/Q_0) vs. (1/T) data were fitted as described in Ref. [24], taking into account the heat transfer from inner surface of cavity to the helium bath [25] using the following equation:

$$R_s(T) = Ae^{-U/T_s} + R_i \tag{6}$$

where R_i refers to residual resistance and Ae^{-U/T_s} is due to the thermally activated quasi-particles in rf field. For weak rf field, the term is a good approximation of the Mattis-Bardeen expression for R_{BCS} [7], where U represents the superconducting gap, T_s is the temperature of cavity's rf surface. The fits were also repeated for with $\sim$ 20 mG trapped residual field. The flux trapping sensitivity $S(n\Omega/mG)$ was calculated as:

$$S = \frac{R_{i,20mG} - R_{i,0mG}}{20} \tag{7}$$

Flux trapping sensitivity as a function of heat treatment temperature followed by $\sim$ 25 μm electropolishing shown in Fig. 3, indicating that the flux trapping sensitivity decreases with increase in heat treatment temperature.

To observe the effect of trapped flux on the performance of the SRF cavities in terms of $Q_o(E_{acc})$, rf measurements were performed after each temperature treatment and applied $\sim$ 0 mG and $\sim$20 mG dc magnetic field prior to each cool-down. Figure 4 (a) and (b) shows the Q_0 vs. E_{acc} after each heat treatment with different flux trapping conditions. Cavity TCA-01 showed some improvement in accelerating gradient as a result of successive heat treatment, however the performance of TE1-05 remains unchanged. The lower accelerating gradient for cavity TCA-01 could be due to the difficulty during the in-house cavity fabrication. The final electron beam welding resulted a hole in cavity equator and was repaired by melting a Nb plug from original Nb sheet. The high field Q-slope started $\sim$ 25 MV/m on both cavities and all tests were limited by quench. Although not shown here, the E_{acc} increases as a result of 120 °C/3h in-situ baking [26].

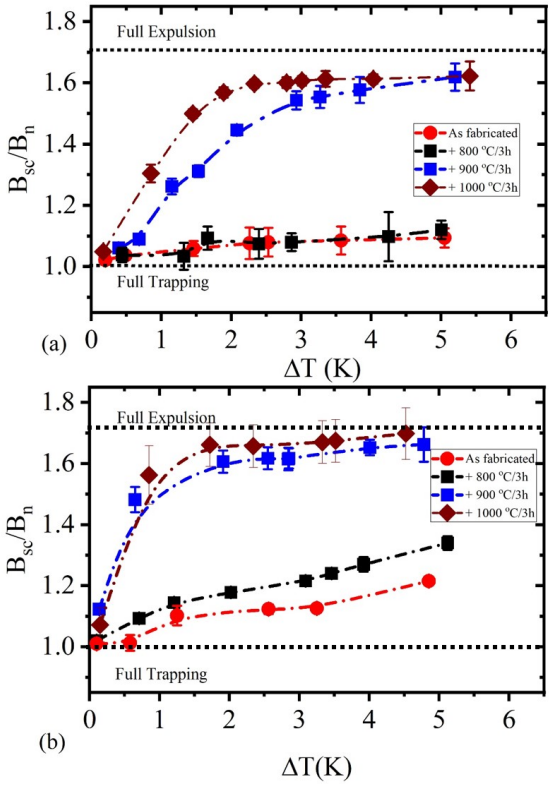

FIGURE 2. Flux expulsion ratio as a function of the temperature difference $\Delta T = T_{top-irirs} - T_{bottom-iris}$ for cavity (a) TCA-01 and (b) TE1-05 after each heat treatment.

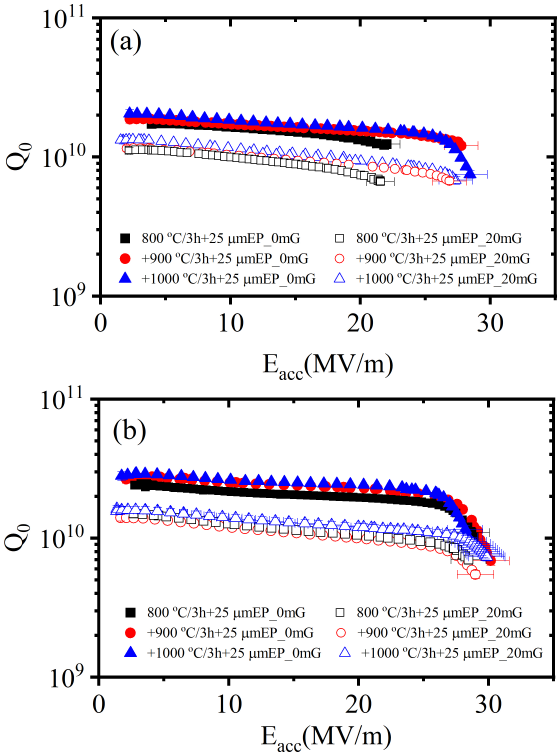

FIGURE 4. Q_0 vs. E_{acc} for cavity (a) TCA-01 and (b) TE1-05 after each successive heat treatment followed by 25 μm inner surface removal by electropolishing with $\sim$ 0 mG and $\sim$20 mG flux trapped respectively. All tests were limited by quench.

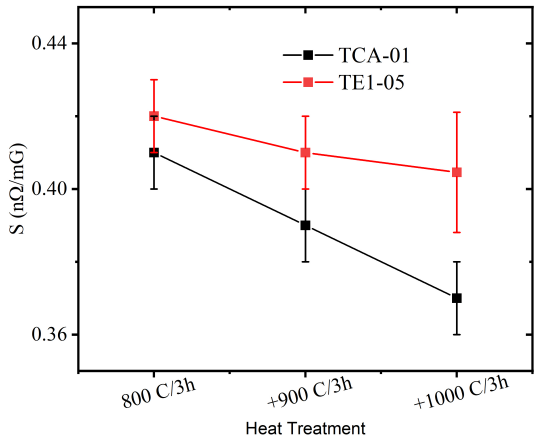

FIGURE 3. Flux trapping sensitivity as a function of heat treatment temperature followed by $\sim$ 25 μm electropolishing.

Sample coupons

Figure 5 shows orientation imaging microscopy images in the normal direction of the Nb sheet of sample coupons from TCA-01 after different heat treatments. Although the average grain size numbers are similar after 800 °C/3h and 900 °C/3h heat treatments, there is variation in aspect ratio of grains. We can clearly see the higher grain size after 1000 °C/3h heat treatment. A full picture of microstructure including grain boundaries, dislocation substructures and local misorientation would be needed to quantify recrystallization and grain growth phenomenon. A study is currently ongoing to analyze the grain growth on sample coupons cut from the cavity half cells. The preliminary results showed that the recrystallization on cavity varies with the degree of deformation during deep drawing process [27].

SUMMARY

The SRF cavities with maximum flux expulsion and minimum flux trapping sensitivity allows us to achieve highly efficient SRF cavities, since the higher quality factor is desirable to operate the high-power particle accelerator in more cost-effective way. The flux expulsion on SRF cavity increases with increase in heat treatment tempera-

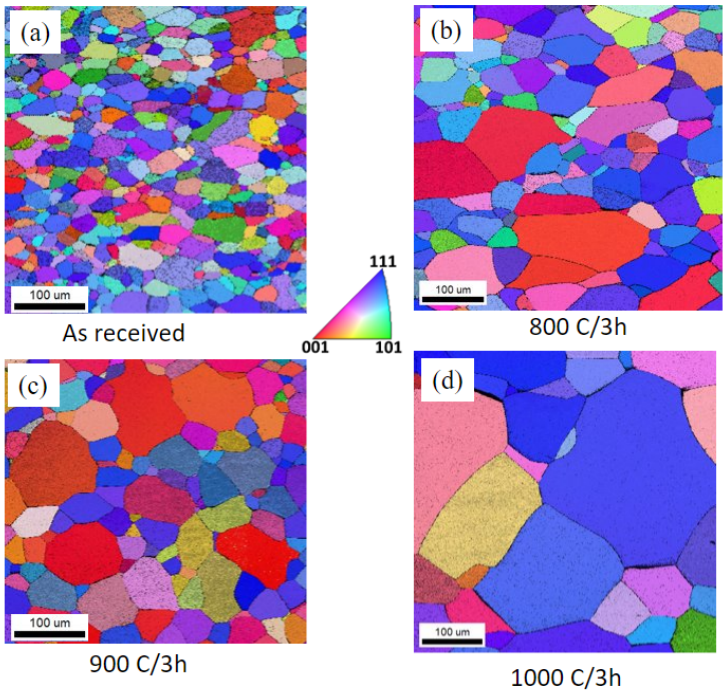

FIGURE 5. IPF map of SRF Nb coupons from TCA-01 (a) as received, (b) 800 °C/3h, (b) 900 °C/3h, and (d) 1000 °C/3h heat treatments.

ture. The flux expulsion ratio shows poor performance after 800 °C/3h heat treatment. Both cavities showed strong flux expulsion behavior after additional 900 °C/3h and additional 1000 °C/3h. The flux trapping sensitivity decreases with increase in heat treatment temperature, likely due to the reduction of the pinning centers [4, 28] and it depends on the final surface preparation prior to the rf test. Recent studies showed that the initial metallurgical state influences the recrystallization behavior and flux expulsion in Nb cavities [29]. The trapped flux can be minimized via different heat treatment, chemical and mechanical polishing, and better cooldown technique and consequently optimize the quality factor. Although, the role of high temperature heat treatment and grain size to the flux expulsion ratio and flux trapping is not fully understood, more analysis of SRF cavities fabricated from different microstructure are under the way.

ACKNOWLEDGMENTS

We would like to acknowledge Dr. Gianluigi Ciovati for support and several discussions. We would like to thank Jefferson Lab technical staff members for cavity fabrication, processing and cryogenic support during rf test. The work is partially supported by the U.S. Department of Energy, Office of Science, Office of High Energy Physics under Awards No. DE-SC 0009960. The manuscript has been authored by Jefferson Science Associates, LLC under U.S. DOE Contract No. DE-AC05-06OR23177.

EDITOR'S NOTE

This manuscript was submitted to the Association of Nepali Physicists in America (ANPA) Conference 2022 for publication in the special issue of Journal of Nepal Physical Society.

REFERENCES

1. P. Dhakal, "Nitrogen doping and infusion in srf cavities: A review," Physics Open **5**, 100034 (2020).
2. M. H. Devoret and R. J. Schoelkopf, "Superconducting circuits for quantum information: an outlook," Science **339**, 1169–1174 (2013).
3. P. Dhakal, "Superconducting radio frequency resonators for quantum computing: A short review," Journal of Nepal Physical Society **7**, 1–5 (2021).
4. P. Dhakal, G. Ciovati, P. Kneisel, and G. R. Myneni, "Superconducting dc and rf properties of ingot niobium," arXiv preprint arXiv:1202.0811 (2012).
5. R. Geng *et al.*, english"SRF Levitation and Trapping of Nanoparticles," in english*Proc. SRF'21*, International Conference on RF Su-

perconductivity No. 20 (JACoW Publishing, Geneva, Switzerland, 2022) pp. 331–335.
6. N. K. Raut, J. Miller, R. Y. Chiao, and J. E. Sharping, "Magnet strength dependence of levitated magnets in a microwave cavity," IEEE Transactions on Instrumentation and Measurement **71**, 1–7 (2022).
7. D. C. Mattis and J. Bardeen, "Theory of the anomalous skin effect in normal and superconducting metals," Physical Review **111**, 412 (1958).
8. J. Bardeen, L. N. Cooper, and J. R. Schrieffer, "Theory of superconductivity," Physical review **108**, 1175 (1957).
9. D. Gonnella *et al.*, "Nitrogen-doped 9-cell cavity performance in a test cryomodule for lcls-ii," Journal of Applied Physics **117**, 023908 (2015).
10. J.-M. Vogt, O. Kugeler, and J. Knobloch, "Impact of cool-down conditions at tc on the superconducting rf cavity quality factor," Physical Review Special Topics-Accelerators and Beams **16**, 102002 (2013).
11. A. Romanenko, A. Grassellino, O. Melnychuk, and D. Sergatskov, "Dependence of the residual surface resistance of superconducting radio frequency cavities on the cooling dynamics around t c," Journal of Applied Physics **115**, 184903 (2014).
12. M. Martinello *et al.*, "Magnetic flux studies in horizontally cooled elliptical superconducting cavities," Journal of Applied Physics **118**, 044505 (2015).
13. J.-M. Vogt, O. Kugeler, and J. Knobloch, "High-q operation of superconducting rf cavities: Potential impact of thermocurrents on the rf surface resistance," Physical Review Special Topics-Accelerators and Beams **18**, 042001 (2015).
14. T. Kubo, "Flux trapping in superconducting accelerating cavities during cooling down with a spatial temperature gradient," Progress of Theoretical and Experimental Physics **2016** (2016).
15. A. Gurevich and G. Ciovati, "Effect of vortex hotspots on the radio-frequency surface resistance of superconductors," Physical Review B **87**, 054502 (2013).
16. P. Dhakal, G. Ciovati, and A. Gurevich, "Flux expulsion in niobium superconducting radio-frequency cavities of different purity and essential contributions to the flux sensitivity," Physical Review Accelerators and Beams **23**, 023102 (2020).
17. S. Posen *et al.*, "Role of magnetic flux expulsion to reach q 0> 3× 10 10 in superconducting rf cryomodules," Physical Review Accelerators and Beams **22**, 032001 (2019).
18. D. Gonnella, J. Kaufman, and M. Liepe, "Impact of nitrogen doping of niobium superconducting cavities on the sensitivity of surface resistance to trapped magnetic flux," Journal of Applied Physics **119**, 073904 (2016).
19. M. Martinello *et al.*, "Effect of interstitial impurities on the field dependent microwave surface resistance of niobium," Applied Physics Letters **109**, 062601 (2016).
20. M. Checchin *et al.*, "Frequency dependence of trapped flux sensitivity in srf cavities," Applied Physics Letters **112**, 072601 (2018).
21. S. Posen *et al.*, "Efficient expulsion of magnetic flux in superconducting radiofrequency cavities for high q0 applications," Journal of Applied Physics **119**, 213903 (2016).
22. S. Balachandran *et al.*, "Direct evidence of microstructure dependence of magnetic flux trapping in niobium," Scientific reports **11**, 1–12 (2021).
23. B. Aune *et al.*, "Superconducting tesla cavities," Physical Review special topics-accelerators and beams **3**, 092001 (2000).
24. G. Ciovati, P. Dhakal, and A. Gurevich, "Decrease of the surface resistance in superconducting niobium resonator cavities by the microwave field," Applied Physics Letters **104**, 092601 (2014).
25. P. Dhakal, G. Ciovati, and G. R. Myneni, "Role of thermal resistance on the performance of superconducting radio frequency cavities," Physical Review Accelerators and Beams **20**, 032003 (2017).
26. B. Khanal and P. Dhakal, "Effect of duration of 120 °c on the performance of superconducting radio frequency niobium cavities," NAPAC'22, Albuquerque, New Mexico, USA, Aug. 2022, paper WEPA27.
27. S. Balachandran *et al.*, "Metallurgical approach to addressing the issue of flux-trapping in nb cavities and the variability found when using nb sheet from different sources," (2020), tESLA Technology Collaboration, Geneva Switzerland.
28. A. S. Dhavale, P. Dhakal, A. A. Polyanskii, and G. Ciovati, "Flux pinning characteristics in cylindrical niobium samples used for superconducting radio frequency cavity fabrication," Superconductor Science and Technology **25**, 065014 (2012).
29. B. Khanal *et al.*, "Magnetic flux expulsion in superconducting radio-frequency niobium cavities made from cold worked niobium," NAPAC'22, Albuquerque, New Mexico, USA, Aug. 2022, paper WEZE5.